AD-A190 824 UNDERLYING BASIS FOR THE EFFECTS OF IRON OXIDATION STATE ON CLAY SWELLING(U) ILLINOIS UNIV AT URBANA J W STUCKI 12 JAN 88 ARO-21652.7-GS DAAG29-84-K-0167 1/1

UNCLASSIFIED F/G 7/2 NL

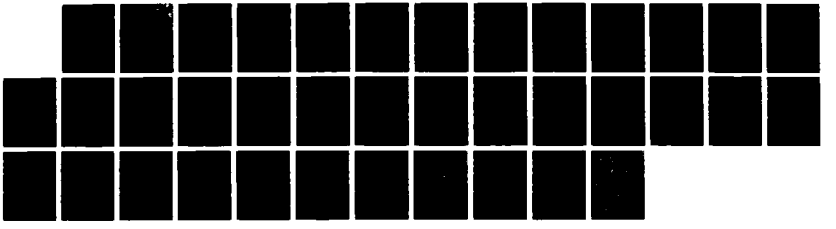

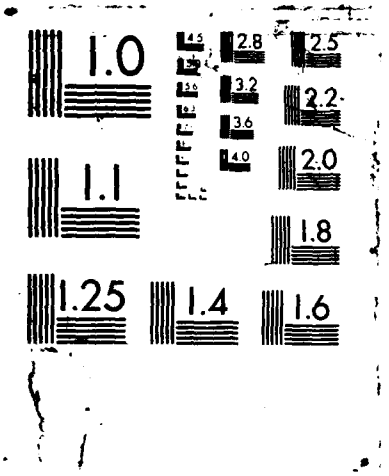
1.0
1.1
1.25
1.4
1.6
1.8
2.0
2.2
2.5
2.8
3.2
3.6
4.0

UNCLASSIFIED

SECURITY CLASSIFICATION OF THIS PAGE

AD-A190 824

REPORT DOCUMENTATION PAGE

DTIC FILE COPY

1b. RESTRICTIVE MARKINGS	
2a. SECURITY CLASSIFICATION AUTHORITY	3. DISTRIBUTION/AVAILABILITY OF REPORT: Approved for public release; distribution unlimited.
2b. DECLASSIFICATION/DOWNGRADING SCHEDULE	
4. PERFORMING ORGANIZATION REPORT NUMBER(S)	5. MONITORING ORGANIZATION REPORT NUMBER(S): ARO 21652.7-65
6a. NAME OF PERFORMING ORGANIZATION: University of Illinois	6b. OFFICE SYMBOL (If applicable):
7a. NAME OF MONITORING ORGANIZATION: U. S. Army Research Office	
6c. ADDRESS (City, State, and ZIP Code): 1102 South Goodwin Avenue, Urbana, Illinois 61801	7b. ADDRESS (City, State, and ZIP Code): P. O. Box 12211, Research Triangle Park, NC 27709-2211
8a. NAME OF FUNDING/SPONSORING ORGANIZATION: U. S. Army Research Office	8b. OFFICE SYMBOL (If applicable):
9. PROCUREMENT INSTRUMENT IDENTIFICATION NUMBER: DAAG29-84-k-0167	
8c. ADDRESS (City, State, and ZIP Code): P. O. Box 12211, Research Triangle Park, NC 27709-2211	10. SOURCE OF FUNDING NUMBERS: PROGRAM ELEMENT NO. / PROJECT NO. / TASK NO. / WORK UNIT ACCESSION NO.

11. TITLE (Include Security Classification): Underlying Basis for the Effects of Iron Oxidation State on Clay Swelling

12. PERSONAL AUTHOR(S): Joseph W. Stucki

13a. TYPE OF REPORT	13b. TIME COVERED	14. DATE OF REPORT (Year, Month, Day)	15. PAGE COUNT
Final	FROM 9-84 TO 9-87	1988 January 12	

16. SUPPLEMENTARY NOTATION: The view, opinions and/or findings contained in this report are those of the author(s) and should not be construed as an official Department of the Army position, policy, or decision, unless so designated by other documentation.

17. COSATI CODES			18. SUBJECT TERMS (Continue on reverse if necessary and identify by block number)
FIELD	GROUP	SUB-GROUP	Clay, Iron, Reduction, Swelling, Water, Microorganisms

19. ABSTRACT (Continue on reverse if necessary and identify by block number)

The effect of Fe(II) in the crystal structure of the clay mineral nontronite on the fraction of clay layers that become completely collapsed was measured directly using a 2-ethoxyethanol surface area technique. Measurements showed that up to 28% of the clay layers became completely collapsed as a result of Fe reduction. X-ray diffraction results also showed that many layers become partially collapsed. Since the combined fraction of these types of layers increased with increasing Fe(II) content in the clay and neither of these types of layers participates in the swelling process, one necessarily concludes that Fe(II) alters swelling by decreasing the number of layers that are capable of full expansion in the presence of water.

20. DISTRIBUTION/AVAILABILITY OF ABSTRACT	21. ABSTRACT SECURITY CLASSIFICATION	
☒ UNCLASSIFIED/UNLIMITED ☐ SAME AS RPT. ☐ DTIC USERS	Unclassified	
22a. NAME OF RESPONSIBLE INDIVIDUAL: Joseph W. Stucki	22b. TELEPHONE (Include Area Code): 217/333-9636	22c. OFFICE SYMBOL

DD FORM 1473, 84 MAR — 83 APR edition may be used until exhausted. All other editions are obsolete.

SECURITY CLASSIFICATION OF THIS PAGE: UNCLASSIFIED

TITLE OF PROJECT: Underlying Basis for the Effects of Iron Oxidation State on Clay Swelling

STATEMENT OF PROBLEM: The objective of this project was to test the hypothesis that the oxidation state of octahedral Fe in the crystal structure of swelling clay minerals affects the number of clay layers that expand and, thereby, the specific surface area and swelling of the clay. A secondary objective was to determine more precisely the empirical relationship between octahedral Fe(II) and the gravimetric water content, m_w/m_c, when the clay is in equilibrium with any swelling pressure, π.

SUMMARY OF RESULTS: The effect of Fe(II) in the crystal structure of the clay mineral nontronite on the fraction of clay layers that become completely collapsed was measured directly using a 2-ethoxyethanol surface area technique. Measurements showed that up to 28% of the clay layers became completely collapsed as a result of Fe reduction. X-ray diffraction results also showed that many layers become partially collapsed. Since the combined fraction of these types of layers increased with increasing Fe(II) content in the clay and neither of these types of layers participates in the

swelling process, one necessarily concludes that Fe(II) alters swelling by decreasing the number of layers that are capable of full expansion in the presence of water.

Ancillary studies associated with this project have also contributed the following:

- A possible method for large-scale, *in situ* alteration of Fe oxidation under field conditions using microorganisms to reduce the Fe.
- The understanding that the effect of Fe(II) on clay swelling is unique to Fe(II) (i.e., does not occur with other divalent ions).
- A better understanding of the electronic and magnetic exchange interactions that occur in the clay crystal structure in the presence of Fe(II).
- An improved and rapid method for determining Fe(II) and total Fe quantitatively in clay minerals.
- Development of methods whereby all of the Fe in an Fe-rich smectite can be reduced, thus opening the way for studies on limits of the effects on minerals and the impact of extensive reduction on mineral integrity.

LIST OF PUBLICATIONS:

1. Effects of iron oxidation state on the specific surface area of nontronite. In Preparation for Submission to **Clays Clay Miner.** Paul R. Lear and Joseph W. Stucki
2. The microbial reduction of iron(III) in clay minerals. **Soil Sci. Soc. Am. J. 51:**1663-1665. Joseph W. Stucki, Peter Komadel, and Henry T. Wilkinson.
3. Intervalence electron transfer and magnetic exchange interactions in reduced nontronite. **Clays Clay Miner. 35:**373-378. Paul R. Lear and Joseph W. Stucki.
4. Mössbauer characterization of iron oxides in nontronite from Hohen Hagen, Federal Republic of Germany. In Press in **Clays Clay Miner.** Paul R. Lear, Peter Komadel, and Joseph W. Stucki.

5. The quantitative assay of minerals for Fe^{2+} and Fe^{2+} using 1,10-phenanthroline. III. A rapid photochemical method. Accepted by **Clays Clay Miner.** Peter Komadel and Joseph W. Stucki.
6. Relationship between surface charge density and swelling of reduced dioctahedral smectites. In Preparation for Submission to **J. Colloid Interface Sci.** Joseph W. Stucki.
7. The magnetic properties of nontronites and site-occupancy of structural Fe. In Preparation for Submission to **Clay Miner.** Paul R. Lear and Joseph W. Stucki.
8. Reduction of structural iron in smectites by microorganisms. In Preparation for Submission to **Soil Sci.** Peter Komadel, Henry T. Wilkinson, and Joseph W. Stucki.
9. Reduction and reoxidation of iron in nontronites. I. Time and temperature dependence and extent of reduction. In Preparation for Submission to **Clays Clay Miner.** Peter Komadel, Paul R. Lear, and Joseph W. Stucki.
10. Reduction and reoxidation of iron in nontronites. II. Questions of reversibility. In Preparation for Submission to **Clays Clay Miner.** Peter Komadel, Paul R. Lear, and Joseph W. Stucki.
11. Biological reduction of structural iron in Na-nontronite. In Press in **Soil Sci. Soc. Am. J.** Jun Wu, Charles B. Roth, and Philip F. Low.
12. *Effects of octahedral iron reduction on* interlayer spacing of Na-nontronite. In Preparation. Jun Wu, Philip F. Low, and Charles B. Roth.

PARTICIPATING SCIENTIFIC PERSONNEL:

Joseph W. Stucki, Associate Professor, University of Illinois
Philip F. Low, Professor, Purdue University
Charles B. Roth, Professor, Purdue University
Jun Wu, Visiting Scientist, Purdue University
Peter Komadel, Visiting Scientist, University of Illinois
Paul R. Lear, Graduate Research Assistant, University of Illinois.

Mr. Lear received a Ph.D. degree from the University of Illinois in June, 1987.

THE EFFECTS OF IRON OXIDATION STATE ON THE SPECIFIC SURFACE AREA OF NONTRONITE[1]

Paul R. Lear and Joseph W. Stucki[2]

[1]Contribution from the Department of Agronomy, University of Illinois, Urbana, IL 61801.

[2]Graduate Research Assistant and Associate Professor of Soil Science, respectively. Current address of the senior author is Department of Chemistry, Michigan State University, East Lansing, MI.

RUNNING HEAD: Effect of Fe(II) on the Surface Area of Nontronite

KEY WORDS: Ferrous, Ferric, Clay, Smectite, 2-ethoxyethanol, Swelling, cation fixation, layer collapse

CORRESPONDING AUTHOR: Joseph W. Stucki
University of Illinois
Department of Agronomy
S-510 Turner Hall
1102 South Goodwin Avenue
Urbana, IL 61801
Phone: (217) 333-9636

Abstract - The effect of Fe oxidation state on the specific surface area, S_m, of nontronite was studied using the < 2 μm, Na^+-saturated fraction of the SWa-1 and Garfield nontronites. The reduction of structural Fe(III) in the octahedral sheet of the nontronite produced a decrease in S_m as measured by the adsorption of 2-ethoxyethanol (EGME). The swellability in water of the nontronite also decreased during reduction. The amount of nonexchangeable Na^+ increased as the extent of reduction increased and was highly correlated to EGME adsorption (r^2 = 0.97).

The relationship between specific surface area and equilibrium water content for the reduced nontronite samples was also determined. This relationship was compared to the theoretical relationship based on the physical model for the swelling of clay particles in water. The decrease in S_m is explained by the collapse of expanded layers to unexpanded layers. The effect of Fe(II) on the swelling of clay in water is, therefore, dependent on the forces which govern layer collapse.

Introduction

In a recent study, Stucki *et al.* (1984b) reported that the swelling of aqueous dispersions of aluminosilicate clay minerals is substantially altered by the oxidation state of octahedral Fe in the clay crystal structure, but all of the factors governing this relationship have yet to be identified. The swelling of clays in their natural oxidation state has been described by Low and coworkers (Odom and Low, 1978; Low and Margheim, 1979; Low, 1980) as a phenomenon deriving from the surface area of the clay, obeying the empirical equation

$$\ln (\Pi + 1) = \alpha/(m_w/m_c) + \ln B, \qquad [1]$$

where Π is the applied swelling pressure; m_w/m_c, the gravimetric water content of the clay in equilibrium with Π; B, a constant that depends on the clay; and α, a function that varies directly with the specific surface area available to water (S_m). Hence, Π varies directly with S_m. The reduced clays studied by Stucki *et al.* (1984c) apparently also obey this equation, so a similar correlation between Π and S_m should exist in reduced clays. If this is true, the specific surface area of reduced clays should be less than in the oxidized state, but such a correlation with S_m has yet to be established.

The specific surface area of swelling clays can be attributed virtually entirely to the planar surfaces of the clay plates. Any change in S_m must, therefore, be accompanied by a loss of planar surfaces. The work of Viani *et al.* (1983, 1985) showed that Π, for a wide variety of swelling clays, is a

single-valued function of the distance, λ_e, between expanding clay layers, and that differences in the swellability of clays is attributable to variations in the relative fraction of expanding *vs.* non-expanding layers rather than to differences in λ_e. The correlation between Π and S_m, therefore, exists because both depend on the same factor, namely, the force or forces governing layer collapse. Results of Viani *et al.* (1983, 1985) also indicate that clay surfaces which participate in swelling are similar in their behavior toward water, regardless of the overall swelling properties of the clay.

For the purposes of the present study, a distinction must be made between completely and partially collapsed layers. The correlation between Π and S_m will deteriorate if the number of partially collapsed layers increases because the swellability of the clay is determined by only those layers which expand fully (Norrish, 1954; Foster *et al.*, 1955; Rhoades *et al.*, 1969), whereas both fully expanded and partially collapsed layers contribute about equally to the surface area. Recent evidence (Wu *et al.*, 1986) indicates that reduced clays possess a greater fraction of partially collapsed ($\lambda < 1.0$ nm) layers than any of the clays studied by Viani *et al.* (1983), so a lower correlation between Π and S_m is expected.

The purpose of the present study was to determine the effect of Fe(II) on S_m, and thereby derive the relationship between Π and S_m in reduced clays; and, further, to examine the implications of such a rela-

tionship on the relative fractions of expanded and partially and completely collapsed layers.

Background

A physical model for the swelling of clay particles in water (Odom and Low, 1978; Low, 1980) consists of n crystallographic layers (~ 1.0 nm thick) oriented parallel. These layers may be subdivided into n-1 elementary layers, each consisting of one interlayer space and half of each clay layer on either side (Figure 1). The mass of interlayer water within one such elementary layer is given by $a_j\lambda_j\rho_j/2$, where a_j is the basal surface area of a single clay layer, λ_j is the distance between the superimposed layers, and ρ_j is the density of the interlayer water. The total mass of water occupying these interlayers, W_i, will be simply the sum of all elementary layers, *viz.*,

$$W_i = \sum_{j=1}^{n-1} a_j\lambda_j\rho_j/2. \qquad [2]$$

Since water may also exist external to the clay crystal, the total mass of water in the clay-water system is given by

$$W_t = W_x + W_i \qquad [3]$$

where W_x is the mass of external water.

The specific surface area, S_j, associated with the planar surfaces of each elementary layer is obtained by dividing a_j by the corresponding mass of clay, m_j, within the elementary layer, giving

$$S_j = a_j/m_j \qquad [4a]$$

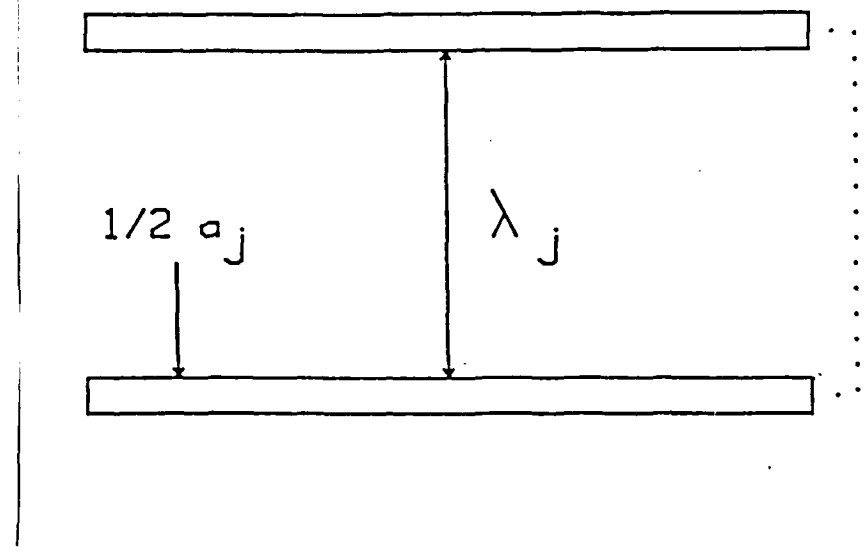

Figure 1. Diagram of two parallel clay layers. The dotted line defines the elementary unit layer, which extends from the center of the upper clay plate across the interlayer space to the center of the lower clay plate. λ_j is the distance separating the plates and a_j is the basal surface area of a single planar surface.

O-218

or

$$a_j = S_j m_j. \qquad [4b]$$

If the mass of the clay layers is uniform, then m_j will be a constant, m, and Eq. [2] can be rewritten, after substituting [4b],

$$W_i = (n-1)\, m \sum_{j=1}^{n-1} S_j \lambda_j \rho_j / 2 \qquad [5]$$

If $n >> 1$, then $(n-1)\, m = m_c$, the total mass of clay, and Eq. [5] can be written

$$W_i = m_c \sum_{j=1}^{n-1} S_j \lambda_j \rho_j / 2 \qquad [6]$$

Equation [3] may be expressed in terms of the mass ratio of water to clay by substituting Eq. [6] for W_i, and dividing by m_c, giving

$$(m_w/m_c)_t = (m_w/m_c)_x + \sum_{j=1}^{n-1} S_j \lambda_j \rho_j / 2. \qquad [7]$$

Equations reported by Odom and Low (1978) and by Low (1980) are special cases of Eq. [7].

For the purposes of the present study, the following simplifications and assumptions are made, which follow previous work of Fink *et al.* (1968), Fink and Nakayama (1972), Odom and Low (1978), and Low (1980):

a) Only three states or types of layers exist (Odom and Low, 1978) in the clay-water system. These layers are designated as collapsed ($\lambda_j = \lambda_u = 0$ nm), partially expanded ($0.2 < \lambda_j = \lambda_p < 1.0$ nm), and fully expanded ($\lambda_j = \lambda_e > 3.0$ nm).

b) The density of water is the same in all interlayers, i.e., ρ_w.

c) Contribution of crystal edges to the total surface area, S_t, is negligible and $n \gg 1$, hence

$$S_t = \sum_{j=1}^{n-1} S_j = S_u + S_p + S_e. \quad [8]$$

And since $f_u + f_p + f_e = 1$ (Odom and Low, 1978), where f is the fraction of layers in the corresponding states, then the following relationships also apply:

$$f_u = S_u/S_t \quad ; \; S_u = f_u S_t \quad [9a]$$

$$f_p = S_p/S_t \quad ; \; S_p = f_p S_t \quad [9b]$$

$$f_e = S_e/S_t \quad ; \; S_e = f_e S_t. \quad [9c]$$

d) Assume S_t equals the theoretical maximum of $8 \cdot 10^6$ cm^2/g.

e) As a consequence of (c),

$$S_m = S_p + S_e = S_t - S_u = (1 - f_u) S_t, \quad [10]$$

where S_m is the available surface area, i.e., that associated with either partially or fully expanded layers.

e) W_x is directly proportional to W_t (Fink *et al.*, 1978), i.e., $W_x = b \cdot W_t$, where b becomes the fraction of total water that exists external to the clay crystal and (1-b) is the fraction within the clay crystal.

Applying these assumptions and simplifications to Eqs. [2] and [3] transforms Eq. [7] to

$$(m_w/m_c)_t = [2(1-b)(1-f_u)]^{-1} \rho_w S_m (f_p \lambda_p + f_e \lambda_e). \quad [11]$$

Note from this relationship that the water content is related to Sm by the factor δ, where

$$\delta = [2(1-b)(1-f_u)]^{-1} \rho_w (f_p \lambda_p + f_e \lambda_e). \quad (12)$$

MATERIALS AND METHODS

The clays used in this study were the < 2 μm fractions of SWa-1 ferruginous smectite (Source Clay Minerals Repository, The Clay Minerals Society) from Grant County, Washington; and Garfield nontronite (API 33-a, Wards Natural Science Establishment). The molecular compositions of these clays are respectively (Goodman *et al.*, 1976; Stucki *et al.*, 1984b)

$$Na_{0.81}(Si_{7.30}Al_{0.70})(Al_{1.06}Fe_{2.73}Mg_{0.26})\,O_{20}(OH)_4$$

and

$$Na_{0.91}(Si_{7.12}Al_{0.88})(Al_{0.19}Mg_{0.11}Fe^{3+}_{3.72}Fe^{2+}_{0.008})\,O_{20}(OH)_4$$

The clays were Na^+ saturated, dialyzed, and freeze-dried.

The reduction of clay suspensions in citrate-bicarbonate buffer solution with sodium dithionite ($Na_2S_2O_4$) salt was accomplished as described by Lear and Stucki (1985) and the swellability in water by the method of Stucki *et al.* (1984c). The specific surface area of clay gels was determined using the method described by Odom and Low (1978), which was patterned after the 2-ethoxyethanol (EGME) method of Carter *et al.* (1965). Implicit to this method is the assumption that EGME wets the same surfaces as water. Freeze-dried samples were equilibrated for

20 days and weighed. Both operations were carried out inside a glove box (Vacuum/Atmospheres Model HE-43 Dri-Lab equipped with a Dri-train) with an atmosphere of less than 10 ppm O_2 to prevent reoxidation of reduced samples. The surface area of the sample was calculated from the ratio of EGME adsorbed relative to Upton montmorillonite, which was assumed to have an ideal surface area of $8 \cdot 10^6$ cm^2/g. EGME is assumed to form a monolayer on all surfaces available to water, thus producing two layers within each partially or fully expanded elementary unit layer of the clay.

Nonexchangeable Na^+ was determined on a series of reduced SWa-1 samples following the procedure of Stucki *et al.* (1984b) for layer charge determinations, except the clay was first washed twice with 20 ml of degassed 1 *M* LiCl, then three times with 30 ml of degassed, distilled deionized H_2O. Iron(II) was measured as described by Stucki (1981) and total Fe by atomic absorption.

RESULTS AND DISCUSSION

As shown in Figure 2, a significant inverse relationship exists between the amount of EGME adsorbed and the Fe(II) content of both the Garfield and SWa-1 nontronite samples, indicating that the oxidation state of Fe has a significant effect on surface properties of the clay. Iron(II) has a similar depressing effect on the water adsorption of these clays (Figure 3).

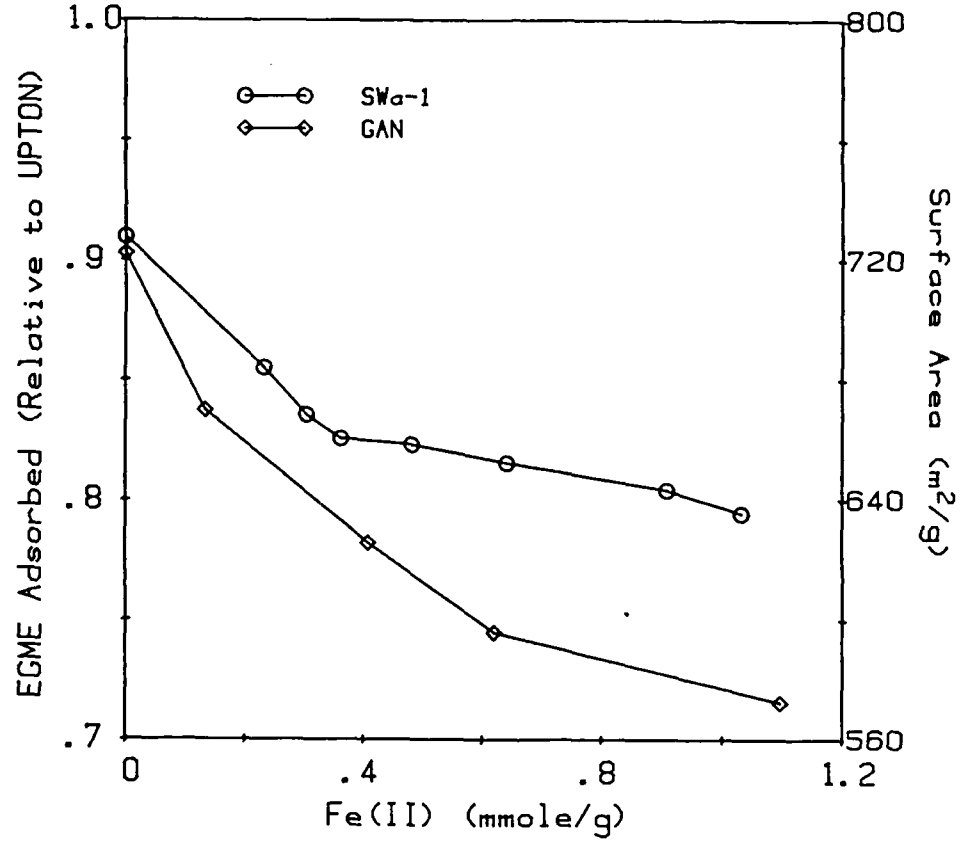

Figure 2. Relationship between the amount of EGME adsorbed relative to Upton montmorillonite (left ordinate) and the corresponding specific surface area, S_m, (right ordinate) *vs.* Fe(II) content of SWa-1 and Garfield nontronite samples.

0-218

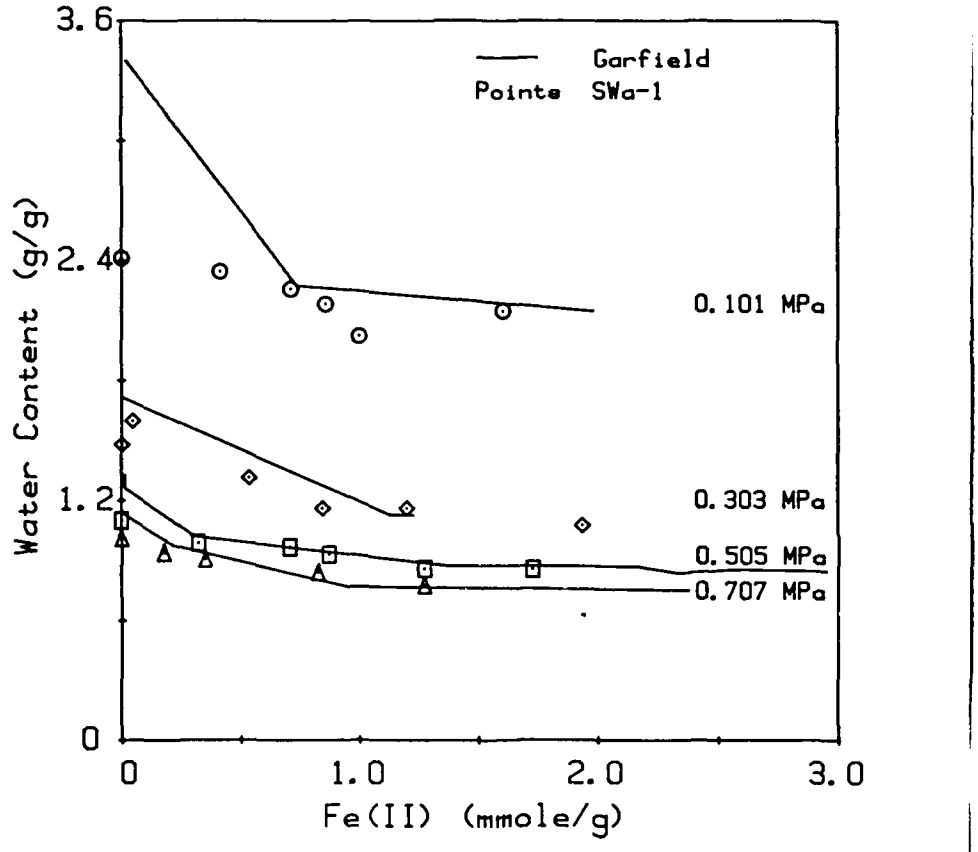

Figure 3. Comparison of observed relationships between the equilibrium water content (m_w/m_c) at four different applied pressures, π, and Fe(II) content of reduced SWa-1 (this study) and Garfield (Stucki *et al.*, 1984b) nontronite samples.

The purpose of conducting EGME adsorption experiments was to determine the specific surface area, S_m, of clays in their water-swollen state as a function of Fe(II) in the clay crystal. The amount of adsorbed EGME will correlate directly with relative values of S_m only if (a) the EGME wets the same surfaces as water, (b) the freeze-dried clay rewets to the same surface area as existed in the original swollen state, and (c) a full monolayer of EGME develops on every available planar surface.

EGME is commonly accepted as capable of wetting the same surfaces as water, so this was presumed in the present study. To determine the effect of freeze-drying on the ability of the clay to rewet, several freeze-dried samples were resuspended in deionized water and their equilibrium water contents determined at 3 MPa applied pressure. The resulting water contents were comparable to values obtained during the first wetting-drying cycle. Condition (b) was, therefore, fulfilled.

Verification of condition (c) was somewhat more difficult, but was also considered fulfilled in this study based on the following observations. Any of the following phenomena would change the amount of EGME adsorbed: i) a rearrangement of clay layers resulting in the complete collapse of some layers and a corresponding decrease in available surface area; ii) a sufficient partial collapse of some clay layers to prevent more than one layer of EGME to enter the elementary unit layer; and iii) a change in the interaction energy between the surface and the adsorbate molecule, which could result in only a single layer or less of EGME within

the elementary unit layer. Occurrence of either ii) or iii) would prevent fulfillment of condition (c) above, and EGME adsorption would underestimate S_m.

To test these possibilities, the extent of counterion fixation was measured and correlated with EGME adsorption. If during Fe reduction some layers collapse completely, a portion of the exchangeable cation will become non-exchangeable or fixed between the layers. Figure 4 illustrates that this does, in fact, occur. As the amount of Fe(II) increased, both the amount of non-exchangeable Na^+ (Table 1) and the fraction of total exchange capacity neutralized by non-exchangeable Na^+ increased. Wu *et al.* (1987) observed a similar effect of Fe oxidation state on K^+ fixation in soils. The fact that some Na^+ was unavailable for exchange by Li^+ indicates that a number of elementary unit layers were unexpanded. And since the fraction of total exchange capacity rendered non-exchangeable was highly correlated with EGME adsorption ($r^2 = 0.97$), the two measurements probably derive from the same phenomenon, i.e., the collapse of fully and/or partially expanded layers to unexpanded layers. Hence, complete layer collapse accounts for most (97%) of the change in EGME adsorption, and ii) and iii) have little importance. It follows, then, that condition (c) is fulfilled and EGME adsorption is an acceptable method to calculate relative values of S_m. This does not preclude the existence of partially expanded layers, but does prove the existence of completely collapsed layers and suggests that most partially expanded

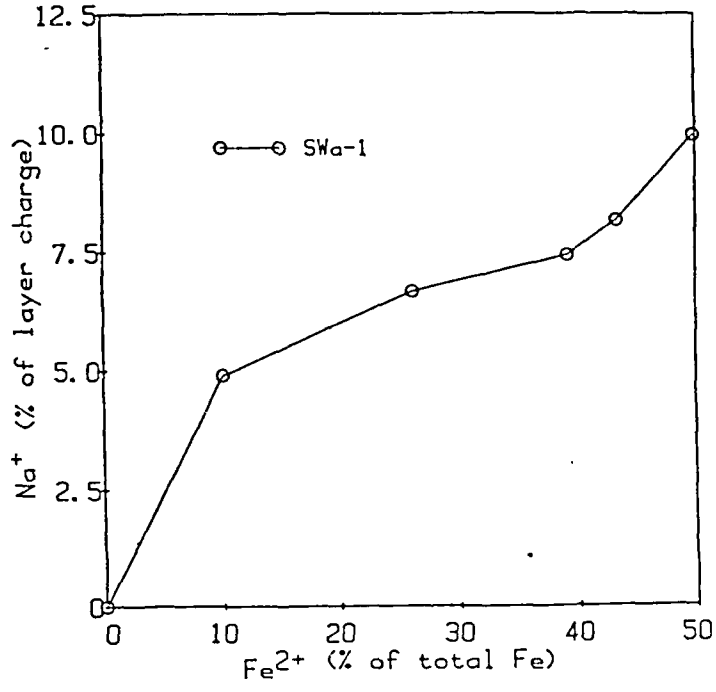

Figure 4. The relationship between the amount of nonexchangeable Na^+, expressed as % of the total layer charge, and Fe(II) content of SWa-1 nontronite sample.

layers still allow entry of two layers of EGME into the elementary unit layer. The nature of the surface itself apparently exhibits little or no attenuation of EGME monolayer adsorption.

The data in Figure 2, therefore, also represent the relative values of S_m, using Upton montmorillonite as 800 m^2/g, and show that the reduction of structural Fe in the crystal structure decreases S_m. This observation is consistent with the adherence of reduced clays to Eq. [1] and with the known effect of Fe(II) on α, π, and m_w/m_c reported by Stucki *et al.* (1984b). Using these values of S_m, the corresponding fractions of unexpanded layers, f_u, in reduced samples were calculated from Eq. [10] and plotted in Figures 6 and 7 for the SWa-1 and Garfield samples, respectively. Notice that the fraction of completely collapsed layers was about 20% or less for both clays over the range of Fe(II) contents studied. Unless these layers are highly ordered in their stacking sequence, they likely will be undetected by the X-ray diffraction methods of Viani *et al.* (1983).

Low (1980) showed for a series of smectites that $(m_w/m_c)_t$, determined at various applied pressures, was approximately proportional to S_m, indicating that δ in Eqs. [11] and [12] was constant for his samples. Similar plots were made for the reduced clays in the present study and are represented in Figure 5 by results obtained at π=0.101 MPa. The value of δ at any value of Fe(II) is given by the slope of the curve at that point. As shown in the Figure, δ was always positive but changed with the Fe(II)

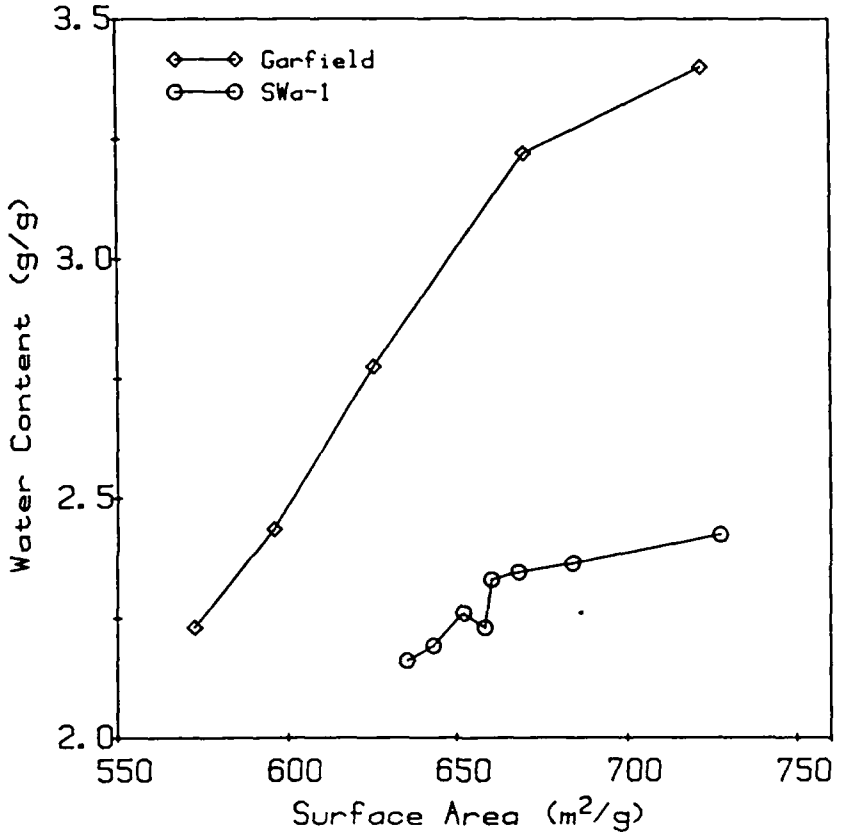

Figure 5. The observed relationship between water content (m_w/m_c) at 0.101 MPa and the specific surface area (S_m). The water contents were determined, by linear regression on the data in Figure 3 for the Fe(II) contents at which the S_m measurements were made.

content of the clay. Statistical analyses of these plots produced approximately equivalent agreement for either a curvilinear or multi-linear regression, but regardless of form, the evidence clearly indicates variation in δ in both clays. Hence, either the assumptions on which Eq. [11] is based are invalid, or one or more of the terms in Eq. [12] varies with Fe(II).

Closer examination of Eq. [12] reveals that δ depends on the fraction (b) of the total water that exists external to the elementary unit layer, the density of interlayer water, and the fractions of and the distances separating partially and fully expanded layers. Notice that since f_u changes (Figures 6 and 7) with Fe(II), values of f_p and f_e must also change because the algebraic sum of all fractions must be unity.

Using Garfield nontronite and following the methods of Viani *et al.* (1983), Wu *et al.* (1986) found that in the range of Fe(II) contents reported in the present study, λ_p and λ_e are approximately 0.95 nm and 7.5 nm, respectively, and independent of Fe(II) content. Assuming a constant value of 1.0 g cm^{-3} for ρ_w, and using measured values of m_w/m_c and S_m, Eq. [11] can, therefore, be solved for f_p at different values of b, giving the relationship

$$f_p = \frac{(m_w/m_c)_t\,(2(1-b)) - \rho_w S_m \lambda_e}{(\lambda_p - \lambda_e)\,\rho_w S_t} \qquad [13]$$

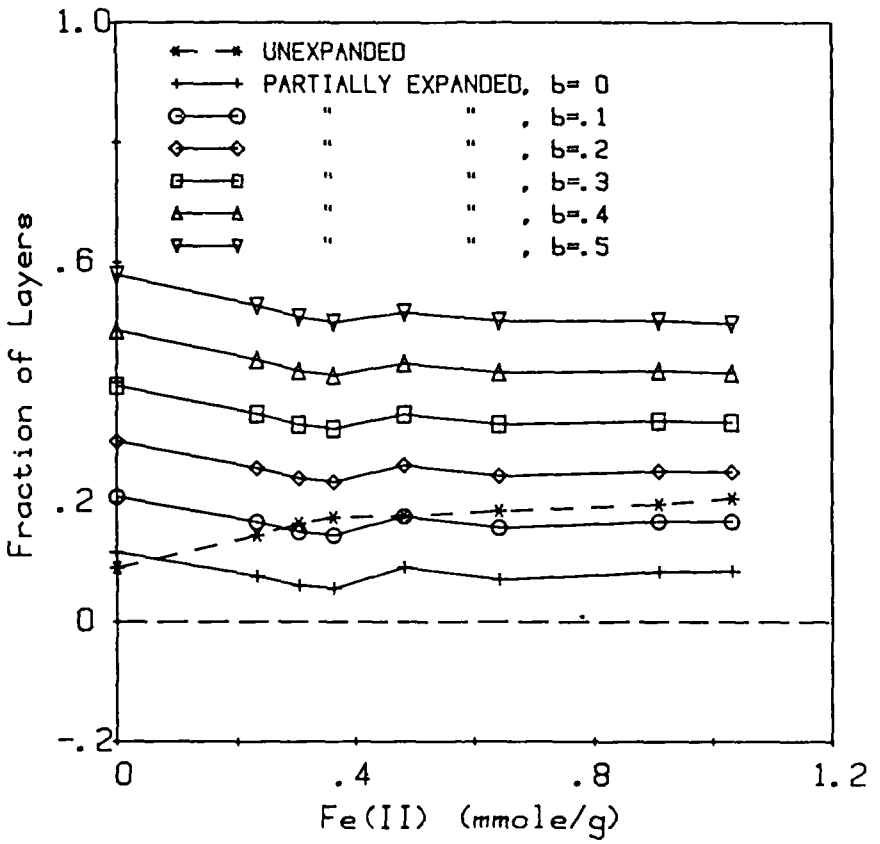

Figure 6. Effect of Fe(II) on the fraction of completely collapsed (unexpanded) and partially expanded layers in the SWa-1 nontronite sample for various values of external water content, b.

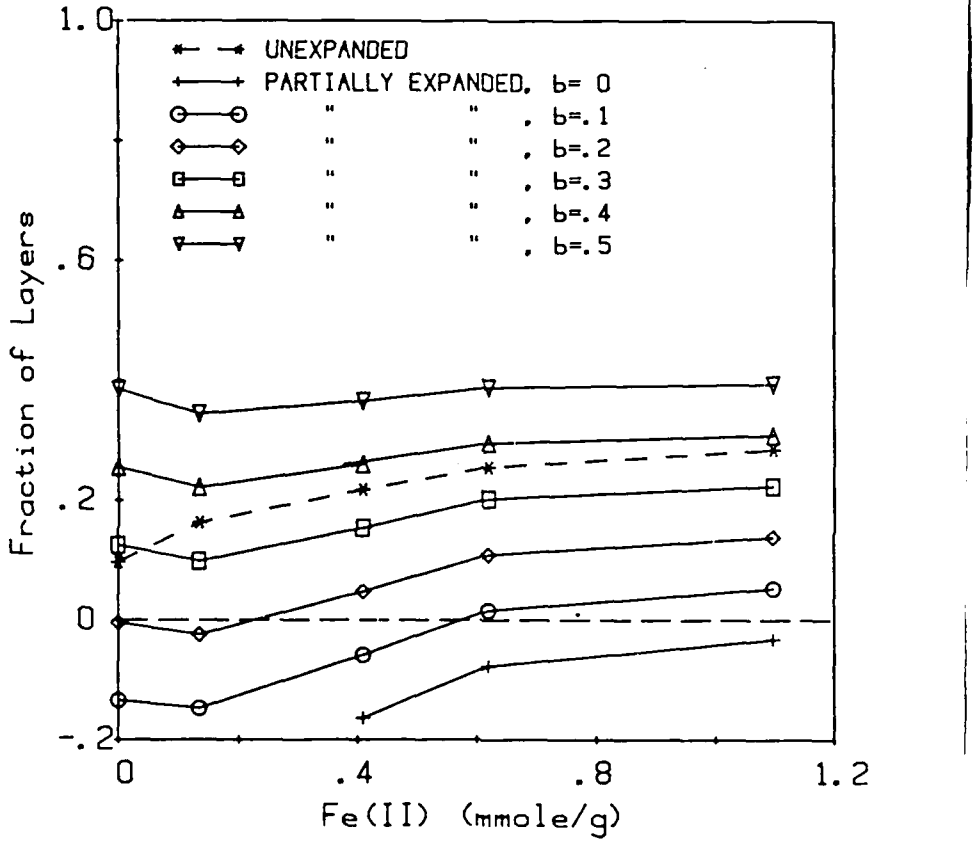

Figure 7. Effect of Fe(II) on the fraction of completely collapsed (unexpanded) and partially expanded layers in the Garfield nontronite sample for various values of external water content, b.

O-218

Figures 6 and 7 were obtained by plotting this equation for different levels of Fe reduction at an applied swelling pressure of 0.101 MPa, and represent the relationship between fraction of partially expanded layers and Fe(II) content of the clays. By substituting the appropriate value of λ_e, plots at other swelling pressures can also be constructed. The value of λ_p apparently is invariant in the range of π and Fe(II) studied here (Wu *et al.*, 1986), but it decreases at higher levels of Fe(II). At very high levels of reduction, λ_e becomes independent of π and varies with Fe(II) only (Wu *et al.*, 1986). Since the actual variation of b with Fe(II) and π is unknown in these samples, such plots as shown in Figures 6 and 7 do not necessarily represent reality but, rather, provide a probable range of allowable values for f_p and b. For example, since $f_p<0$ is illogical, only those values of b which produce $f_p\geq 0$ are allowed. Consequently, at least 20% (b=.2) of the water in the oxidized Garfield sample (Fe(II)=0) must be external to the interlayer space at equilibrium with an applied pressure of .101 MPa (Figure 7). Only at higher levels of reduction can the external water content be lower. The value of b=0 is allowed in the SWa-1 sample, however. If b is unaffected by Fe(II), values of f_p change only slightly with increasing Fe(II) and the observed variation in m_w/m_c is accounted for entirely by the change in f_u. But notice that the value of f_p is very sensitive to b. Further conclusions must await the measurement of b at various levels of reduction and swelling pressures, at which time the actual relationship between f_p and Fe(II) can be determined.

In summary, the above discussion reveals that the specific surface area of swelling clays decreases with increasing Fe(II) in the octahedral sheet and that up to 20 and 28% of the layers become completely collapsed in the SWa-1 and Garfield samples, respectively. Completely collapsed layers are coexistent with partially and fully expanded layers, the relative fractions of which depend slightly on the level of reduction and more significantly on the fraction of water in the clay that is external to the interlayer space. The specific forces governing the collapsing of layers are still unidentified, but are manifested in the decrease of both the specific surface area and the swellability in water of the reduced nontronite samples. The effect of Fe(II) on clay swelling, therefore, has now been clearly identified with the forces governing layer collapse.

REFERENCES

1. Carter, D. L., M. D. Heilman, and C. M. Gonzalez. 1965. Ethylene glycol monoethyl ether for determining surface area of layer silicate minerals. **Soil Sci. 100:**356-360.
2. Fink, D. H., C. I. Rich, and G. W. Thomas. 1968. Determination of internal surface area, external water, and amount of montmorillonite in clay-water systems. **Soil Sci. 105:**71-77.
3. Fink, D. H. and F. S. Nakayama. 1972. Equation for describing the free-swelling of montmorillonite in water. **Soil Sci. 114:**325-332.

4. Foster, W. R., J. G. Savins, and J. M. Waite. 1955. Lattice expansion and rheological behavior of relationships in water-montmorillonite systems. p. 296-316. *In.* Ada Swineford (ed.) **Clays Clay Minerals. Proc. 3rd Natl. Conf., Houston, Texas, 1954. Natl. Acad. Sci. Natl. Res. Coun. Publ. 395.**

5. Goodman, B. A., J. D. Russell, A. R. Fraser, and F. W. D. Woodhams. 1976. A Mössbauer and I.R. spectroscopic study of the structure of nontronite. **Clays Clay Miner. 24:**53-59.

6. Lear, P. R., and J. W. and Stucki. 1985. Role of structural hydrogen in the reduction of iron in nontronite. **Clays Clay Miner. 33:**539-545.

7. Low, P. F. 1980. The swelling of clay: II. Montmorillonites. **Soil Sci. Soc. Am. J. 44:**667-676.

8. Low, P. F., and J. F. Margheim. 1979. The swelling of clay. I. Basic concepts and empirical equations. **Soil Sci. Soc. Am. J. 43:**473-481.

9. Norrish, K. 1954. The swelling of montmorillonite. **Disc. Faraday Soc. 18:**120-134.

10. Odom, J. W., and P. F. Low. 1978. Relationship between swelling, surface area and b dimension of Na-montmorillonites. **Clays Clay Miner. 26:**345-351.

11. Rhoades, J. D., R. D. Ingvalson, and H. T. Stumpf. 1969. Interlayer spacing of expanded clay minerals at various swelling pres-

sures: an X-ray diffraction technique for direct determination. **Soil Sci. Soc. Am. J. 33:**473-475.

12. Stucki, J. W., D. C. Golden, and C. B. Roth. 1984. Effects of reduction and reoxidation of structural iron on the surface charge and dissolution of dioctahedral smectites. **Clays Clay Miner. 32:**350-356.

13. Stucki, J.W., P. F. Low, C. B. Roth, and D. C. Golden. 1984. Effects of oxidation state of octahedral iron on clay swelling. **Clays Clay Miner. 32:**357-362.

14. Stucki, J. W. 1981. The quantitative assay of minerals for Fe^{2+} and Fe^{3+} using 1,10-phenanthroline: II. A photochemical method. **Soil Sci. Soc. Am. J. 45:**638-641.

15. Viani, B. E., P. F., Low, and C. B. Roth. 1983. Direct measurement of the relation between interlayer force andinterlayer distance int he swelling of montmorillonite. **J. Colloid Interface Sci. 96:**229-244.

16. Viani, B. E., C. B. Roth, and P. F. Low. 1985. Direct measurement of the relation between swelling pressure and interlayer distance in Li-vermiculite. **Clays Clay Miner. 33:**244-250.

17. Wu, J., P. F. Low, and C. B. Roth. 1986. Effects of octahedral iron reduction on interlayer spacing of Na-nontronite. **Clay Mineral Society Abstracts 1986:**43.

the 1.0-nm peak will need to be resolved in terms of the mechanism and products of illite degradation by alkylammonium cations.

Whenever the alkylammonium method of determining layer charge is used with clay samples, the possibility of errors from the K^+-depletion of illite should be anticipated. The extent of illite K^+-depletion will depend on the nature of the illite, the length of the alkylamine hydrochloride treatments, and other experimental conditions. The incidence of this problem, however, can be clearly identified by determining the amounts of K^+ extracted by the treatments.

REFERENCES

Badraoui, M., P.R. Bloom, and R.H. Rust. 1987. The occurrence of high-charged beidellite in a Vertic Haplaquoll of northwestern Minnesota. Soil Sci. Soc. Am. J. 51:813–818.

Brindley, G.W. 1966. Ethylene glycol and glycerol complexes of smectites and vermiculites. Clay Miner. 6:237–259.

Kunze, G.W. 1965. Pretreatments for mineralogical analysis. *In* C.A. Black et al. (ed.) Methods of soil analysis, Part 1. Agronomy 9:568–597.

Lagaly, G., and A. Weiss. 1969. Determination of the layer charge in mica-type layer silicates. p. 61–80. *In* L. Heller (ed.) Proc. Int. Clay Conf., Tokyo, Japan. Israel Univ. Press. Jerusalem.

Laird, D.A. 1987. Layer charge and crystalline swelling of expanding 2:1 phyllosilicates. Ph.D. diss. Iowa State Univ., Ames.

Laird, D.A., T.E. Fenton, and A.D. Scott. 1985. Clay mineral transformations and selective translocations in an Argialboll-Argiaquoll sequence. Agron. Abstr. American Society of Agronomy, Madison, WI, p. 231.

Lim, C.H., and M.L. Jackson. 1982. Dissolution for total elemental analysis. *In* A.L. Page et al. (ed.) Methods of soil analysis. Part 2. 2nd ed. Agronomy 9:1–11.

Mackintosh, E.E., and D.G. Lewis. 1968. Displacement of potassium from micas by dodecylammonium chloride. Trans. Int. Congr. Soil Sci. 9th. 2:695–703.

Mackintosh, E.E., D.G. Lewis, and D.J. Greenland. 1971. Dodecylammonium-mica complexes: I. Factors affecting the exchange reaction. Clays Clay Miner. 19:209–218.

Mackintosh, E.E., D.G. Lewis, and D.J. Greenland. 1972. Dodecylammonium-mica complexes: II. Characterization of the reaction products. Clays Clay Miner. 20:125–134.

Mehra, O.P., and M.L. Jackson. 1960. Iron oxide removal from soils and clays by a dithionite-citrate system buffered with sodium bicarbonate. Clays Clay Miner. 7:317–327.

Rühlicke, G. 1985. Layer charge of clay minerals in K fixing sedimentary soils. Potash Rev. 4/83 8.

Rühlicke, G., and E.E. Kohler. 1981. A simplified procedure for determining layer charge by the n-alkylammonium method. Clay Miner. 16:305–307.

Rühlicke, G., and E.A. Niederbudde. 1985. Determination of layer-charge density of expandable 2:1 clay minerals in soils and loess sediments using the alkylammonium method. Clay Miner. 20:291–300.

Senkayi, A.L., J.B. Dixon, L.R. Hossner, and L.A. Kippenberger. 1985. Layer charge evaluation of expandable soil clays by an alkylammonium method. Soil Sci. Soc. Am. J. 49:1054–1060.

Theissen, A.A., and M.E. Harward. 1962. A paste method for preparation of slides for clay mineral identification by x-ray diffraction. Soil Sci. Soc. Am. Proc. 26:90–91.

Weiss, A. 1963. Mica-type layer silicates with alkylammonium ions. Clays Clay Miner. 10:191–224.

Microbial Reduction of Structural Iron(III) in Smectites[1]

JOSEPH W. STUCKI, PETER KOMADEL, AND HENRY T. WILKINSON[2]

ABSTRACT

Octahedral Fe(III) in the crystal structures of three different smectites was reduced to Fe(II) by actively growing microorganisms indigenous to the clay. The smectites were SWa-1 ferruginous smectite from Grant County, Washington; API 33a, Garfield Nontronite; and API 25, Upton montmorillonite. Bacterial growth was supported by incubating clay suspensions at room temperature in a nutrient broth solution consisting of peptone and beef extract. Some samples were first sterilized (by autoclaving), then seeded with bacteria that had been isolated previously from the SWa-1 sample. The effect of O_2 on microbial reduction of Fe(III) was also tested. Results revealed that, in all three clays, about 0.30 mmol Fe(III)/g clay was reduced to Fe(II) by bacteria in a 28-day period. The specific organism responsible for Fe reduction has yet to be classified, but it was more efficient in samples that had not been purged of O_2, and it appears to be indigenous to the SWa-1 clay.

Additional Index Words: **bacteria, Fe reduction, clay minerals, nontronite, montmorillonite, aerobic, anaerobic.**

Stucki, J.W., P. Komadel, and H.T. Wilkinson. 1987. Microbial reduction of structural iron(III) in smectites. Soil Sci. Soc. Am. J. 51:1663–1665.

[1] Contribution from the Dep. of Agronomy, Univ. of Illinois, S-510 Turner Hall, 1102 South Goodwin Avenue, Urbana, IL 61801. Received 25 Feb. 1987.

[2] Associate Professor of Soil Science, Visiting Scientist, and Assistant Professor of Soil Ecology, respectively, Dep. of Agronomy, Univ. of Illinois, Urbana, IL 61801. Permanent address of the second author is Institute of Inorganic Chemistry, Center of Chemical Research, Slovak Academy of Sciences, 84236 Bratislava, Czechoslovakia.

OF ALL THE ELEMENTS comprising the crystal structures of clay minerals, Fe is one of the most interesting because it may be oxidized or reduced in situ. Oxidation state is significant because it affects a number of physicochemical properties of clays (Foster, 1953; Kohyama et al., 1973; Stucki et al., 1984c; Stucki, 1987), which are of great importance to many disciplines of science and in various agricultural, industrial, and engineering applications. Changes in oxidation state occur during important natural processes such as mineral weathering and water-logging of soils and sediments. In virtually all of the studies where changes in Fe oxidation state have been investigated, the Fe was reduced by chemical reagents such as hydrazine (Rozenson and Heller-Kallai, 1976a; Stucki and Roth, 1977), sodium disulfide (Rozenson and Heller-Kallai, 1976b), or sodium dithionite (Rozenson and Heller-Kallai, 1976a; Stucki and Roth, 1977; Russell et al., 1979). The probability that any of these reducing agents is a significant factor in naturally occurring processes is extremely low, so one cannot be certain that the aforementioned relationships between Fe oxidation state and clay properties are actually invoked by natural redox reactions. The reduction of Fe(III) to Fe(II) by bacteria and other commonly occurring microorganisms (Halvorson and Starkey, 1927; Starkey and Halvorson, 1927; Roberts, 1947) has been demonstrated with Fe in solution (Takai and Kamura, 1966), in chelates (Cox, 1980), and in oxides (Ottow,

persisted throughout the entire incubation period. The slight reoxidation during days 6 to 14 (B, Fig. 1) is likely the result of exhaustion of reduction potential from the NB suspension, combined with some residual dissolved O_2 in the system. In the treatment containing nonsterilized clay, microbial reoxidation of Fe also may have occurred, but direct evidence is lacking. Whether the Fe(III)-reducing bacterium, P-1, also oxidizes Fe(II) under certain conditions is unclear. Further, soils are routinely autoclaved twice, on two consecutive days, to ensure complete sterilization. After only one autoclave cycle, as in the present experiments, surviving microorganisms could reduce a small amount of Fe(III), but analysis of experimental control samples indicated that this quantity was insignificant (Fig. 2).

After 28 d of incubation, the fraction of total Fe reduced was 11.3%. The steady increase in Fe(II) is attributed to the activity of bacteria indigenous to the clay. Curve A (Fig. 1) actually represents the net reduction due to all processes occurring in the system. Since curve B represents the combined effect of NB and dissolved O_2, subtracting B from A gives the net reduction due to microbes (C, Fig. 1). The net result is 8.2% reduction of total Fe after 28 d and 11% after 71 d (not shown). The rate of reduction was greatest during the first 3 d, which then leveled to a very low rate. These levels of reduction are sufficient to produce substantial changes in clay properties (Stucki et al., 1984b, 1984c).

The presence of dissolved O_2 in the system has at least two possible effects: first, as seen above in the sterilized sample (B, Fig. 1), some reoxidation occurs; and, second, the efficiency of the organism(s) depends on whether it is aerobic or anaerobic, which in turn will dictate the most favorable environment. In an experiment to test the effects of O_2, some samples were purged with N_2 prior to incubation in order to minimize any effect of dissolved O_2. For sterilized samples, the level of Fe reduction was initially much greater (B, Fig. 2) than in unpurged samples (B, Fig. 2), indicating that a substantial amount of reoxidation offsets the reductive influences of NB and bacteria during the initial incubation period. Over 28 d, the amount of Fe(II) remained about constant in the purged sample. When the same experiment was performed using unsterilized clay (A, Fig. 2), the net efficiency of the organism(s) at reducing Fe was much greater when O_2 was present initially, in spite of some reoxidation. Cell counts showed less microbial growth in the purged (1×10^8 CFU/mL) than in the unpurged (1×10^{10} CFU/mL) sample after 4 d, which confirms the relationship between CFU and Fe reduction. It is possible that the net Fe reduction observed is due to the combined effects of anaerobic and aerobic bacteria.

Experiments were expanded to include Upton montmorillonite and Garfield nontronite. In these experiments, the P-1 organism, seeded into sterile samples of all three clays, produced (Table 1) similar levels of reduction as observed by incubating the unsterilized SWa-1 clay. Over half of the total Fe in Upton was reduced. On the basis of absolute levels of reduction, however, the extent of reduction was comparable in all three clays.

In summary, three simultaneous processes are occurring in the clay–NB system: (i) reduction of the clay by the components of NB; (ii) reoxidation of the clay by dissolved O_2 in the system; and (iii) microbial reduction of structural Fe in the clay, which is the dominant effect. Indigenous organisms, when provided a nutrient source, successfully reduced structural Fe(III). The specific organism responsible for this reduction (P-1) has yet to be classified, but it appears to be indigenous to the SWa-1 clay.

ACKNOWLEDGMENT

The authors gratefully acknowledge financial support of this research from the Illinois Agric. Exp. Stn. and the U.S. Army Res. Office (Contract no. DAAG29-84-k-0167). We also acknowledge the work of Patrick J. Getty, Undergraduate Special Problems Student, Univ. of Illinois, who isolated the P-1 organism.

REFERENCES

Cox, C.D. 1980. Iron reductases from *Pseudomonas aeruginosa*. J. Bacteriology 141:199–204.

Fischer, W.R. 1987. Microbiological reactions of iron in soils. p. 715–748. *In* J.W. Stucki et al., (ed) Iron in soils and clay minerals. D. Reidel Publ., Dordrecht, Netherlands.

Foster, M.D. 1953. Geochemical studies of clay minerals: II. Relation between ionic substitution and swelling in montmorillonites. Am. Mineral. 38:994–1006.

Halvorson, H.O., and R.L. Starkey. 1927. Studies on the transformations of iron in nature. II. Theoretical considerations. J. Phys. Chem. 31:626–631.

Kohyama, N., S. Shimoda, and T. Sudo. 1973. Iron-rich saponite (ferrous and ferric forms). Clays Clay Miner. 21:229–237.

Münch, J.C., and J.C.G. Ottow. 1977. Model experiments on the mechanism of bacterial iron-reduction in water-logged soils. Z. Pflanzenernaehr. Bodenkd. 140:549–562.

Münch, J.C., and J.C.G. Ottow. 1982. Effect of cell contact and iron(III) oxide form on bacterial iron reduction. Z. Pflanzenernaehr. Bodenkd. 145:66–77.

Ottow, J.C.G. 1982. Significance of redox potentials for reduction of nitrate and iron(III) oxides in soils. Z.Pflanzenernaehr. Bodenkd. 145:91–93.

Roberts, J.L. 1947. Reduction of ferric hydroxide by strains of *Bacillus polymyxa*. Soil Sci. 63:134–140.

Rozenson, I., and L. Heller-Kallai. 1976a. Reduction and oxidation of Fe^{3+} in dioctahedral smectites. 1: Reduction with hydrazine and dithionite. Clays Clay Miner. 24:271–282.

Rozenson, I., and L. Heller-Kallai. 1976b. Reduction and oxidation of Fe^{3+} in dioctahedral smectites. 2: Reduction with sodium sulphide solutions. Clays Clay Miner. 24:283–288.

Russell, J.D., B.A. Goodman, and A.R. Fraser. 1979. Infrared and Mössbauer studies of reduced nontronites. Clays Clay Miner. 27:63–71.

Starkey, R.L., and H.O. Halvorson. 1927. Studies on the transformations of iron in nature. II. Concerning the importance of microorganisms in the solution and precipitation of iron. Soil Sci. 24:381–402.

Stucki, J.W. 1981. The quantitative assay of minerals for Fe^{2+} and Fe^{3+} using 1,10-phenanthroline. II. A photochemical method. Soil Sci. Soc. Am. J. 45:638–641.

Stucki, J.W. 1987. Structural iron in smectites. p. 625–675. *In* J.W. Stucki et al. (ed.) Iron in soils and clay minerals. D. Reidel Publ., Dordrecht, Netherlands.

Stucki, J.W., D.C. Golden, and C.B. Roth. 1984a. The preparation and handling of dithionite-reduced smectite suspensions. Clays Clay Miner. 32:191–197.

Stucki, J.W., D.C. Golden, and C.B. Roth. 1984b. Effects of reduction and reoxidation of structural iron on the surface charge and dissolution of dioctahedral smectites. Clays Clay Miner. 32:350–356.

Stucki, J.W., P.F. Low, C.B. Roth, and D.C. Golden. 1984c. Effects of oxidation state of octahedral iron on clay swelling. Clays Clay Miner. 32:357–362.

Stucki, J.W., and C.B. Roth. 1977. Oxidation-reduction mechanism for structural iron in nontronite. Soil Sci. Soc. Am. J. 41:808–814.

Takai, Y., and T. Kamura. 1966. The mechanism of reduction of waterlogged paddy soil. Folia Microbiol. (Prague) 11:304–313.

Clays and Clay Minerals, Vol. 35, No. 5, 373–378, 1987

INTERVALENCE ELECTRON TRANSFER AND MAGNETIC EXCHANGE IN REDUCED NONTRONITE

PAUL R. LEAR AND JOSEPH W. STUCKI

Department of Agronomy, University of Illinois
Urbana, Illinois 61801

Abstract—The effects of chemical reduction of structural Fe^{3+} in nontronite SWa-1 (ferruginous smectite) on intervalence electron transfer (IT) and magnetic exchange were investigated. Visible absorption spectra in the region 800–400 nm of a chemical reduction series of the SWa-1 nontronite revealed an IT band near 730 nm (13,700 cm^{-1}). Both the intensity and position of this band were affected by the extent of Fe reduction. The intensity increased until the Fe^{2+} content approached 40% of the total Fe, then decreased slightly with more Fe^{2+}. The position of the band also shifted to lower energy as the extent of reduction increased.

Variable-temperature magnetic susceptibility measurements showed that the magnetic exchange in unaltered nontronite is frustrated antiferromagnetic, but ferromagnetic in reduced samples. Magnetic ordering temperatures are in the range 10–50 K, depending on the extent of reduction. The ferromagnetic component in the magnetization curve increased with increasing Fe^{2+} in the crystal structure. The positive paramagnetic interaction likely is due to electron charge transfer from Fe^{2+} to Fe^{3+} through such structural linkages as Fe^{2+}–O–Fe^{3+} (perhaps following a double exchange mechanism), which is consistent with the visible absorption spectra.

Key Words—Intervalence electron transfer, Iron, Magnetic susceptibility, Nontronite, Reduction, UV-visible spectroscopy.

INTRODUCTION

As reviewed by Stucki (1987), the oxidation state of Fe in smectites affects many important clay properties, but the molecular reactions and mechanisms governing these relationships are poorly understood. To understand better the specific processes that occur, the present study was undertaken to examine the changes in optical (electronic) and magnetic properties of nontronite that accompany chemical reduction of structural Fe^{3+}. The visible spectra (800–400 nm) of both unaltered and reduced nontronite samples were obtained to identify the intervalence electron transfer (IT) transitions and to determine the effect of Fe^{2+} content on the intensity of the IT transitions. Magnetic susceptibility and magnetization measurements were used to assess the magnetic ordering and exchange interactions.

BACKGROU[illegible]

Intervalence electron transfer

In any mixed-valence compou[illegible] of the type $A^{n+}B^{m+}$, the potential exists for an electr[illegible] in the B site to transfer to the A site, creating $A^{(n+1)+}$. Mineralogical examples of mixed-valence compou[illegible]ds include magnetite, ilvaite, and vivianite. Such in[illegible]valence electron transfer can be used to enhance understanding of the properties of mixed-valence minerals, whether naturally occurring or chemically produced.

IT transitions in minerals are observed as charge-transfer bands in the optical spectra of minerals containing Fe^{2+} and Fe^{3+} in their crystal structures (Hush, 1967). The reduction of structural Fe^{3+} in nontronite results in a color change from yellow to green or blue-green. This green or blue-green color has been identified as a charge-transfer transition and attributed to the presence of Fe^{2+} and Fe^{3+} in the mineral structure (Anderson and Stucki, 1979).

IT transitions occur via vibronic coupling of two states in a mixed-valence system (Schatz, 1980). Vibronic coupling may be understood as the overlap of the vibrational potential energy wells of two symmetrical states, i.e., ($Fe^{3+}Fe^{2+}$) and ($Fe^{2+}Fe^{3+}$), and is illustrated by the vibrational potential energy diagram presented in Figure 1 for electron transfer in one of the normal modes (i.e., an internal molecular coordinate along which an independent vibration of the molecule occurs) of the system. The particular normal mode of the potential energy wells shown is intended to represent the symmetrical breathing mode involving Fe–O at a given Fe center. The potential energy wells for the two states are displaced from one another because the Fe^{2+}–O equilibrium distance differs from the Fe^{3+}–O distance. By virtue of vibronic coupling, the electron transfer between Fe centers occurs through a vibrationally excited state (B^*) of the molecule rather than through an electronically excited state, and the electronic ground state for ($Fe^{3+}Fe^{2+}$) is the same as for ($Fe^{2+}Fe^{3+}$). The amount of optical excitation required for the transition ($E_{op} = E_{B^*} - E_A$) depends on the equilibrium displacement, or difference in the position, of the two potential energy curves. The difference is

referred to as the vibronic (or electron-phonon) coupling parameter and is denoted by λ. The point of intersection (B) between the two curves defines the classical energy of activation required for thermal electron transfer ($E_{th} = E_B - E_A$). For a symmetrical mixed-valence system, E_{op} exceeds E_{th} by a factor of 4 (Hush, 1967).

Magnetic ordering

Magnetic ordering is the directional alignment of atomic magnetic moments due to interactions between atomic centers. In materials which order magnetically, spontaneous ordering occurs only if the sample is below some critical temperature (which varies widely among minerals) such that the magnetic interactions overcome random fluctuations. In phyllosilicates, magnetic ordering is due to the presence of paramagnetic ions in the crystal structure, mainly high-spin Fe^{3+} and Fe^{2+} which have atomic magnetic moments due to five and four unpaired electrons, respectively. In iron-rich minerals such as nontronite, the type of exchange coupling between magnetic cations on adjacent sites determines whether the moments of neighboring cations are aligned parallel (↑↑) or antiparallel (↑↓). The method of exchange via an intervening anion (i.e., a shared O^{2-}) is called superexchange (Kramers, 1934; Anderson, 1950, 1959). In oxides and clay minerals, the Fe^{2+}–O–Fe^{2+} exchange interactions are often ferromagnetic with the atomic moments aligned parallel, and Fe^{3+}–O–Fe^{3+} exchange interactions are generally antiferromagnetic, with the moments aligned antiparallel (Goodenough, 1963; Ballet and Coey, 1982). For mixed-valent Fe^{2+}–O–Fe^{3+} pairs, the magnetic coupling is ferromagnetic and may be due to a charge-transfer process called double exchange (Zener, 1951).

MATERIALS AND METHODS

Materials

The nontronite used in this experiment was the <2-μm fraction of ferruginous smectite SWa-1 (Source Clay Minerals Repository of The Clay Minerals Society) from Grant County, Washington. It has a total Fe content of 20.08% (3.595 mmole/g) and a structural formula according to Goodman *et al.* (1976), of:

$$Na_{0.78}(Si_{7.30}Al_{0.70})(Al_{1.06}Fe_{2.74}Mg_{0.26})O_{20}(OH)_4.$$

No Fe was assigned to tetrahedral sites because, even though Mössbauer work by Goodman *et al.* (1976) reported small amounts in nontronites SWa-1 (6% of total Fe) and Garfield (9% of total Fe), a more recent study by Bonnin *et al.* (1985), employing a variety of spectroscopic techniques, cast doubt on the presence of tetrahedral Fe in these nontronites. Further, room-temperature Mössbauer spectra of sample SWa-1 (Lear and Stucki, unpublished), in which the c* axis of the sample was oriented at 54.7° relative to the γ-ray, required only two octahedral Fe^{3+} doublets to obtain a statistically acceptable fit ($\chi^2 = 0.92$ with 3 million counts per channel). The clay was Na^+-saturated, dialyzed, and freeze-dried before use.

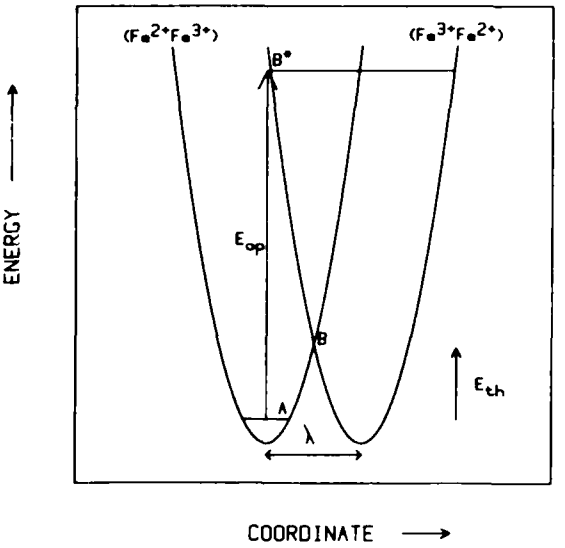

Figure 1. Vibrational potential energy vs. configurational coordinate for electron transfer via vibronic coupling between two symmetrical states of a single oscillator. A, initial state; B*, vibrationally excited state; B, thermally excited state; λ, vibronic coupling parameter; E_{op}, optical transition energy; E_{th}, thermal transition energy. Energy of initial state (left-hand well) is same as final (right-hand well) state (from Hush, 1967).

Methods

Suspensions of sample SWa-1 in a citrate-bicarbonate (C-B) buffer solution were chemically reduced with sodium dithionite ($Na_2S_2O_4$) salt as described by Lear and Stucki (1985). Ferrous iron was determined as described by Stucki (1981); total Fe was determined by atomic absorption.

All visible spectra were measured at room temperature using a Beckman model 5230 UV-visible spectrophotometer equipped with a scattered transmission accessory. A peristaltic pump circulated the clay suspension (2.2 mg of clay/ml) through a flow cell to keep the colloids suspended. The scattered transmission accessory virtually eliminated possible light-scattering differences that were due to variations in particle size among samples. Magnetic susceptibility and magnetization measurements were obtained using a SQUID (superconducting quantum interfering device) magnetometer from SHE Industries for powders of both the reduced and nonreduced nontronite samples.

RESULTS AND DISCUSSION

Stucki *et al.* (1984) recently reported that treatment with C-B solution removes significant amounts of Al

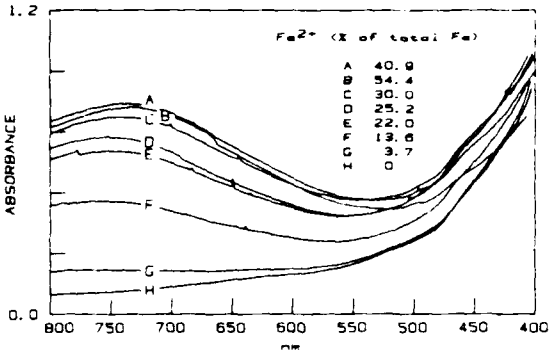

Figure 2. Visible absorption spectra for reduced and unaltered suspensions of sample SWa-1 (2.2 mg clay ml) in the region 800–400 nm. Inset reports Fe^{2+} content of samples as percentage of total Fe.

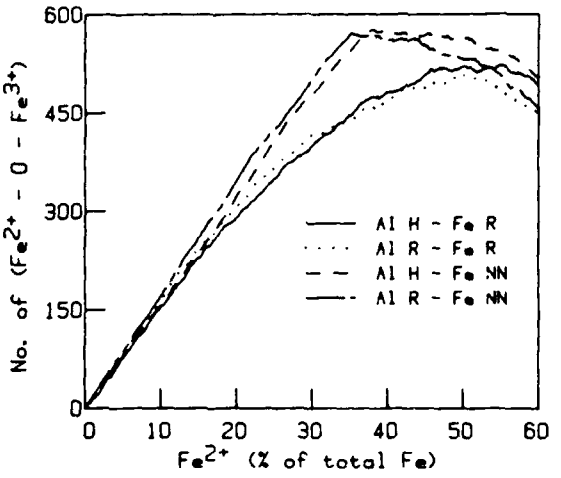

Figure 3. Predicted relationship between number of Fe^{2+}–O–Fe^{3+} linkages and Fe^{2+} content based on computer simulation. Distribution patterns for diamagnetic ions (represented by Al) used were homogeneous (H) and random (R); distribution patterns for Fe^{2+} were random (R) and nearest-neighbor restricted (NN).

and lesser amounts of Fe and Si from clay structures. They suggested, therefore, that some properties of samples reduced with dithionite in C-B could be artifacts of dissolution rather than consequences of Fe reduction. In the present study, the effect of this treatment on optical spectra and magnetic susceptibility was determined by comparing an unaltered sample with a C-B treated sample. No difference was observed in the visible spectrum, and the magnetic susceptibility, although shifted slightly in magnitude, exhibited the same type of exchange interaction in both samples (A and B, Figure 5). Observed differences between unaltered and reduced nontronite, therefore, were attributed to the effect of Fe oxidation state.

Intervalence electron transfer

The IT transition in reduced sample SWa-1 was noted as a broad band centered near 730 nm (13,700 cm^{-1}), which increased in intensity as the Fe^{2+} content increased, then decreased slightly as Fe^{2+} exceeded 40% of the total Fe (B, Figure 2). The center of the band also shifted to lower wavelength as the extent of reduction increased. This band is actually a composite of many individual transitions of Gaussian lineshape, in which the distribution of these transitions determines the position and the profile of the band. The change in position of the maximum as the degree of reduction increased suggests that the distribution of individual IT transitions shifts toward higher energy as more Fe^{2+} is introduced into the mineral structure (Table 1). This shift is especially noticeable if the Fe^{2+} content exceeds 25% of the total Fe (compare C and D, Figure 2).

Table 1. Intensity and position of intervalence electron transfer band for reduced and unaltered SWa-1 samples.

Sample	Fe (% of total Fe)	Position (nm)	Intensity (a.u.)
A	40.9	736	0.835
B	54.4	727	0.816
C	29.1	739	0.778
D	25.2	746	0.700
E	22.0	750	0.643
F	13.7	750	0.451
G	3.7		0.182
H	0		0.096

a.u. = absorbance units (arbitrary).
No discernible maximum. Intensity listed was determined at 750 nm.

The intensity of the IT band increased directly with Fe^{2+} content (experimental points in Figure 4; Table 1) until about Fe^{2+} = 40% of the total Fe. At this Fe^{2+} content, the intensity decreased slightly (cf. spectra A (40.9% Fe^{2+}) and B (54.4% Fe^{2+}) in Figure 2), thereby suggesting that the absorbance of the IT band is a direct reflection of the number of Fe^{2+}–O–Fe^{3+} entities, which reach a theoretical maximum at Fe^{2+} = 50% of the total Fe. Substantial conversion of Fe^{2+}–O–Fe^{3+} to Fe^{2+}–O–Fe^{2+} at Fe^{2+} contents > 50% of the total Fe would produce a non-linear intensity response, because the Fe^{2+}–O–Fe^{2+} groups do not contribute to the IT process. The formation of Fe^{2+}–O–Fe^{3+} in the structure is governed by the probability of Fe^{2+} in adjacent sites, which in turn depends on the distribution pattern by which Fe^{2+} is introduced into the Fe^{3+} matrix (i.e., with or without nearest-neighbor restrictions) and on the distribution of diamagnetic ions in the structure.

A computer method was developed to simulate the Fe^{2+} vs. intensity relationship. In the simulation model, the intensity was represented by the number of Fe^{2+}–O–Fe^{3+} moieties and the dioctahedral sheet consisted

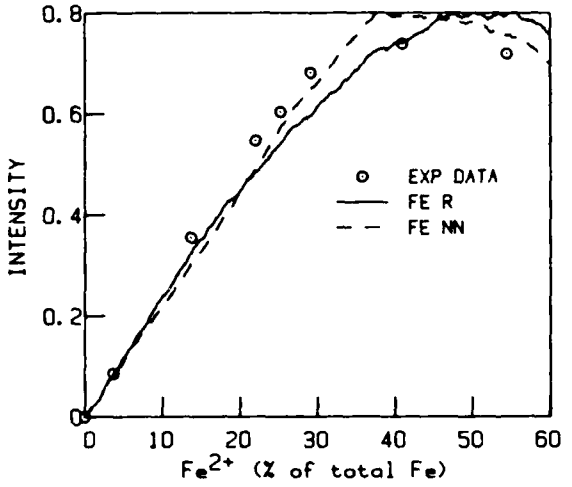

Figure 4. Comparison of observed intensity of the intervalence electron transfer band (O) relative to the unaltered nontronite SWa-1 with the intensity predicted by computer simulations with random (——) and nearest neighbor restricted (- - - -) distribution patterns for Fe^{2+}. Determination coefficients (r^2) were .96 and .99, respectively.

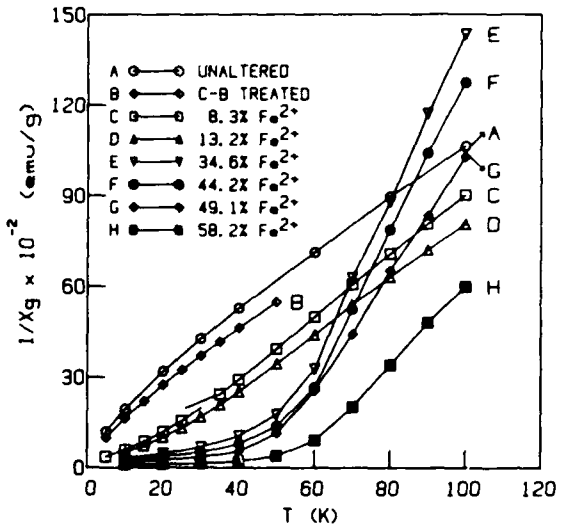

Figure 5. $1/\chi$ vs. T for reduced and unaltered SWa-1 powder samples obtained at 0.1 tesla. Curie-Weiss Law parameters, obtained from the linear portion of the curves, are listed in Table 2.

of 1600 cations distributed centrosymmetrically, i.e., 1200 Fe^{3+} ions and 400 diamagnetic (e.g., Al^{3+}, Mg^{2+} represented by Al) ions. Distribution schemes for the Al ions were either random or homogeneous. A random distribution pattern was used for the conversion of Fe^{3+} to Fe^{2+} during the reduction simulation, with either no restrictions (denoted R), or a nearest-neighbor restriction (denoted NN) which precluded Fe^{2+}–O–Fe^{2+} linkages until no other combinations were possible.

The data in Figure 3 suggest that the diamagnetic ion distribution (homogeneous or random) had little influence on the Fe^{2+}–O–Fe^{3+} vs. Fe^{2+} relationship. A marked difference, however, was noted between the two Fe^{3+}-reduction patterns. With no restrictions (R), the number of Fe^{2+}–O–Fe^{3+} linkages followed Fe^{2+} nonlinearly, whereas simulation with the nearest-neighbor restriction (NN) was close to linear until a critical value was reached (about 35–37% of the total Fe), beyond which the restriction could no longer be enforced. A comparison of these line shapes with the actual measured intensities (Figure 4) indicates that the NN model more closely matched the experimental results than the R model. The critical value in the model is less than 50% of the total Fe because of the presence of diamagnetic ions. A typical average environment around Fe^{2+} likely includes one Al and two Fe^{3+} ions at the critical value.

Magnetic exchange interactions

Based on the inverse susceptibility plots ($1/\chi$ vs. T) (Figure 5), samples can be divided naturally into four groups: A and B, C and D, E and F, and G and H, which correspond to degrees of reduction of 0%, 8–14%, 34–44%, and 49–58% of total Fe, respectively. All plots were analyzed using the Curie-Weiss law, $1/\chi = (T - \theta)/C$, in which χ is the measured susceptibility, C is the Curie constant, and θ is the Curie-Weiss paramagnetic temperature. The values of C and θ (Table 2) were obtained from the slope and x-intercept ($1/\chi = 0$), respectively, of the linear extrapolation of $1/\chi$ vs. T.

The first group consists of the unaltered (A) and C-B treated (B) SWa-1 samples. The value of $\theta = -19$ K for the unaltered sample is comparable to those reported previously of -20 K (Bonnin, 1981) and -27 K (Ballet and Coey, 1982). The negative value indicates that Fe^{3+}–O–Fe^{3+} exchange is antiferromagnetic. Plots of magnetization (M) vs. magnetic field (H) at 5 K for sample (A) are also characteristic of antiferromagnetic exchange (Figure 6). The failure of $1/\chi$ to increase sharply at low T (Figure 5) indicates that long-range magnetic ordering is absent, suggesting either chemical disorder or "frustration." The presence and distribution of diamagnetic cations could produce chemical disorder in the octahedral sheet by separating the magnetic cations into small, isolated clusters, thus preventing long-range ordering. Alternatively, "frustration" would occur if the immediate Fe neighbors of another Fe atom were neighbors of each other, thus precluding simultaneous satisfaction of all antiferromagnetic exchange, i.e., if two adjacent moments were aligned anti-parallel (↑↓), the third could not align anti-parallel to both. Hence, the system would be "frus-

Table 2. Curie constants (C) and Curie-Weiss temperature (θ) determined for reduced and unaltered nontronite samples.

Fe^{2+} (% of total Fe)	C (emu mole K)	θ (K)
0	9.11	−19.2
8.3	8.02	11.0
13.2	8.92	12.3
34.6	2.97	47.8
44.2	3.22	49.3
49.1	4.22	46.9
58.2	6.31	53.6

trated." Similar conclusions can be drawn for the C-B treated sample. The effects of chemical disorder and frustration on long-range magnetic ordering in nontronites will be discussed in more detail by Lear and Stucki in a forthcoming publication.

A possible alternative explanation for the magnetic behavior of samples A and B is superparamagnetism. Superparamagnetic behavior at such low temperatures, however, is unlikely because of the large particle size of the clay mineral relative to known superparamagnetic minerals, such as ferrihydrite (Coey and Readman, 1973).

The other three groups (C and D, E and F, and G and H) in Figure 5 are comprised of reduced samples. As Fe^{3+} in the octahedral sheet is converted to Fe^{2+}, Fe^{2+}–O–Fe^{3+} pairs form to produce ferromagnetic interactions which lead to positive paramagnetic Curie temperatures of about 10 to 55 K, depending on the extent of reduction (Figure 5; Table 2). The magnetization curve for a reduced (Fe^{2+} = 22% of the total Fe) sample at 5 K (Figure 6) also indicates the presence of ferromagnetic interactions, showing the rapid saturation which is characteristic of a ferromagnet.

Samples C and D are slightly reduced and contain small amounts of Fe^{2+} in a Fe^{3+} structure, resulting in small domains of Fe^{2+}–O–Fe^{3+}. The susceptibility is dominated by the frustrated antiferromagnetic component seen in A and B, but the ferromagnetic component is sufficiently prominent to produce positive Curie-Weiss temperatures (Table 2). The moderately reduced samples (E and F) are dominated by ferromagnetic exchange in Fe^{2+}–O–Fe^{3+}. The amount of Fe^{2+} is sufficient (about 30–45% of the total Fe) that only a few unreduced domains remain in the structure. Finally, samples G and H have sufficiently large Fe^{2+} contents that Fe^{2+}–O–Fe^{2+} linkages form at the expense of Fe^{2+}–O–Fe^{3+}. The Fe^{2+}–O–Fe^{2+} linkages introduce an additional ferromagnetic component. The NN model for the distribution of Fe^{2+} dictates that these linkages occur only in highly reduced samples (Fe^{2+} > 35% of the total Fe).

As stated above, ideally Fe^{2+}–O–Fe^{3+} linkages exhibit antiferromagnetic exchange; i.e., at the magnetic ordering temperature the lowest energy state is that in

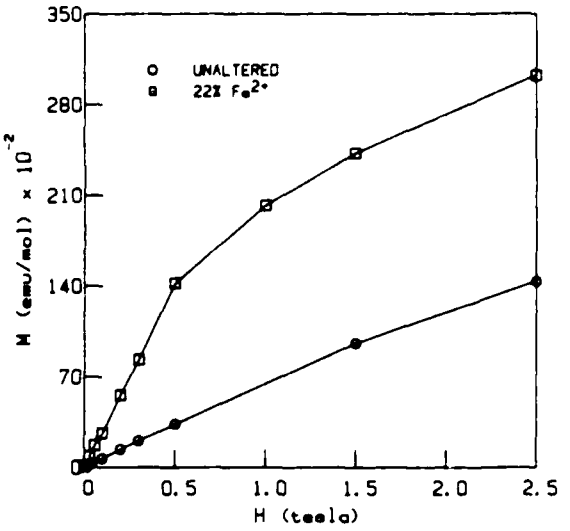

Figure 6. Magnetization curves at 5 K for reduced (Fe^{2+} = 22% of total Fe) and unaltered SWa-1 samples.

which the atomic magnetic moments on adjacent Fe atoms are aligned antiparallel. If a single Fe atom becomes reduced, however, the lowest energy state for magnetic ordering is that in which the non-exchanged electrons are aligned parallel, leading to ferromagnetic exchange. The inclusion of the extra electron due to reduction, therefore, causes a rearrangement in the relative positions of the energy levels for Fe–O–Fe linkages. This observed ferromagnetic exchange in the reduced sample suggests that the double exchange mechanism (Zener, 1951) may occur if Fe^{2+}–O–Fe^{3+} exchange takes place. This exchange involves the transfer of one electron, without changing spin, from Fe^{2+} to the shared O^{2-} ion and the simultaneous transfer of an electron with parallel spin from O^{2-} to Fe^{3+} (Figure 7). This double exchange can occur only if the non-exchanged electrons on the Fe atoms are aligned parallel, otherwise the exchange would violate the Pauli exclusion principle (i.e., any pair of electrons in an orbital must be aligned antiparallel) and thus be forbidden. Therefore, Zener's mechanism of double-exchange favors parallel alignment of spins of adjacent cations, leading to ferromagnetic exchange.

SUMMARY AND CONCLUSIONS

The reduction of structural Fe^{3+} in nontronite SWa-1 suggests a model in which Fe^{2+} is randomly distributed in a centrosymmetric Fe^{3+} matrix, with the restriction that no Fe^{2+}–O–Fe^{2+} pairs form until all possible Fe^{2+}–O–Fe^{3+} combinations have been made. Visible absorption spectra indicate that the prominent IT band at about 730 nm arises from electron charge transfer via vibronic coupling of Fe^{2+} and Fe^{3+} in adjacent octahedral sites, bridged through an O^{2-} ligand. Magnetic

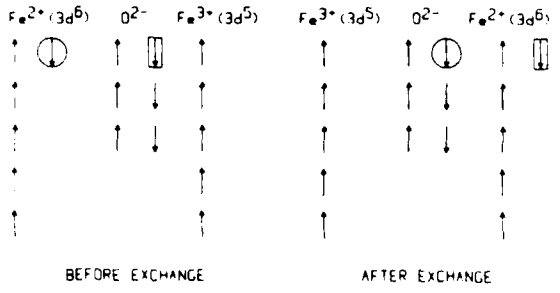

Figure 7. Proposed mechanism to account for the ferromagnetic coupling for a mixed-valence system (Zener, 1951). Exchanged electrons are indicated by enclosure in either a circle or rectangle.

exchange between Fe^{3+} ions were antiferromagnetic, but the presence of chemical disorder or frustration inhibited long-range ordering. The introduction of Fe^{2+} by chemical reduction produced a ferromagnetic component due to Fe^{2+}–O–Fe^{3+}. An additional ferromagnetic component, due to Fe^{2+}–O–Fe^{2+} interactions, was seen at higher levels of reduction (Fe^{2+} >35% of the total Fe).

ACKNOWLEDGMENTS

The authors gratefully acknowledge financial support of this project by the U.S. Army Research Office (Contract No. DAAG29-84-k-0167), and the Illinois Agricultural Experiment Station.

REFERENCES

Anderson, P. W. (1950) Antiferromagnetism. The theory of superexchange interaction. *Phys. Rev.* **79**, 350–356.

Anderson, P. W. (1959) New approach to the theory of superexchange interaction. *Phys. Rev.* **115**, 2–13.

Anderson, W. L. and Stucki, J. W. (1979) Effect of structural Fe^{2+} on visible absorption spectra of nontronite suspensions. in *Proc. Int. Clay Conf., Oxford, 1978*, M. M. Mortland and V. C. Farmer, eds., Elsevier, Amsterdam, 75–83.

Ballet, O. and Coey, J. M. D. (1982) Magnetic properties of sheet silicates, 2:1 layer minerals. *Phys. Chem. Miner.* **8**, 218–229.

Bonnin, D. (1981) Propriétés magnétiques liées aux désordres bidimensionnels dans un silicate lamellaire ferrique: La nontronite: These d'Etat, Université de Paris, 82 pp.

Bonnin, D., Calas, G., Suquet, H., and Pezerat, H. (1985) Sites occupancy of Fe^{3+} in Garfield nontronite: A spectroscopic study. *Phys. Chem. Minerals* **12**, 55–64.

Coey, J. M. D. and Readman, P. W. (1973) Characterisation and magnetic properties of natural ferric gel. *Earth Planet. Sci. Letters* **21**, 45–51.

Goodenough, J. B. (1963) *Magnetism and the Chemical Bond*. Interscience, New York, 393 pp.

Goodman, B. A., Russell, J. D., Fraser, A. R., and Woodhams, F. W. D. (1976) A Mössbauer and I.R. spectroscopic study of the structure of nontronite. *Clays & Clay Minerals* **24**, 53–59.

Hush, N. S. (1967) Intervalence transfer absorption. Part 2. Theoretical considerations and spectroscopic data. in *Progress in Inorganic Chemistry*, F. A. Cotton, ed., Interscience, New York, 357–390.

Kramers, H. A. (1934) L'interaction entre les atomes magnétogènes dans un cristal paramagnétique. *Physica* **1**, 182–192.

Lear, P. R. and Stucki, J. W. (1985) Role of structural hydrogen in the reduction and reoxidation of iron in nontronite. *Clays & Clay Minerals* **33**, 539–545.

Schatz, P. N. (1980) A vibronic coupling model for mixed-valence compounds and its application to real systems. in *Mixed-Valence Compounds*, D. B. Brown, ed., D. Reidel, Boston, 115–188.

Stucki, J. W. (1981) The quantitative assay of minerals for Fe^{2+} and Fe^{3+} using 1,10-phenanthroline. II. A photochemical method. *Soil Sci. Soc. Amer. J.* **45**, 638–641.

Stucki, J. W. (1987) Structural iron in smectites. in *Iron in Soils and Clay Minerals*, J. W. Stucki, B. A. Goodman, and U. Schwertmann, eds., D. Reidel, Dordrecht, 625–675.

Stucki, J. W., Golden, D. C., and Roth, C. B. (1984) Effects of reduction and reoxidation of structural iron on the surface charge and the dissolution of dioctahedral smectites. *Clays & Clay Minerals* **32**, 350–356.

Zener, C. (1951) Interaction between the *d* shells in the transition metals. *Phys. Rev.* **81**, 440–444.

Received 2 February 1987, accepted 24 March 1987. Ms 1639

END

DATE

FILMED

5-88

DTIC